Electronic Supplementary Material (ESI) for New Journal of Chemistry.

Anchored and Confined Pt Nanoparticles in Radial Mesoporous Hollow Carbon Spheres Enhancing Oxygen Reduction Reaction Stability

Lijuan Cao[a,b,c], Hongwei Zhu[a], Yadong Li[a,b,c], Chen Yang[a], Xilong Wang[a], Han-Pu Liang[a,b,c,*]

[a] Key Laboratory of Biofuels, Qingdao Institute of Bioenergy and Bioprocess Technology, Chinese Academy of Sciences, No.189 Songling Road, Qingdao 266101, P. R. China

[b] Sino-Danish College, University of Chinese Academy of Sciences, No. 380 Huaibeizhuang, Huairou district, Beijing 101408, P. R. China

[c] Sino-Danish Centre for Education and Research, No. 380 Huaibeizhuang, Huairou district, Beijing 101408, P. R. China

[*]Corresponding Author. E-mail: lianghp@qibebt.ac.cn (H.-P. Liang)

Experimental section

Materials and chemicals. Tetraethyl orthosilicate (TEOS), formaldehyde (37 wt%), and chloroplatinic acid hexahydrate ($H_2PtCl_6 \cdot 6H_2O$) were purchased from Aladdin. Ammonia ($NH_3 \cdot H_2O$), resorcinol, ethanol, hydrofluoric acid (HF), ethylene glycol, and nitric acid (HNO_3, 65 wt%) were obtained from Sinopharm Chemical Reagent Beijing Co., Ltd. 5 wt% Nafion ionomer was bought from Sigma-Aldrich. Commercial Pt/C (20 wt%) was purchased from Johnson Matthey. Vulcan XC-72R was bought from Cabot Corporation.

Characterization. Scanning electron microscopy (SEM) images were taken on a Hitachi S4800 field-emission SEM microscope. Transmission electron microscopy (TEM) measurements were conducted on a Hitachi H-7650. High resolution transmission electron microscopy (HRTEM), high-angle annular dark-field scanning transmission electron microscope (HAADF-STEM) images, and energy dispersive X-ray (EDX) mapping images were obtained from a JEOL LEM 2200FS/TEM. N_2 adsorption-desorption isotherms were measured on Micromeritics ASAP 2460. The powder X-ray diffraction (XRD) data were obtained from a Bruker D8-Advance X-ray diffractometer. Raman spectra were collected on a Thermo DXR spectrometer system. N_2 adsorption-desorption isotherms were measured on Micromeritics ASAP 2460 analyzer. Chemical compositions of catalysts were analyzed by X-ray photoelectron spectroscopy (XPS). The contents of Pt in the catalysts were obtained from inductively coupled plasma optical emission spectroscopy (Agilent, ICP-OES).

Electrochemical measurements. The activity of catalysts for the oxygen reduction reaction (ORR) was evaluated by rotating disc electrodes (RDE) with a three-electrode system. A platinum wire, $Hg/HgSO_4$, and a glassy carbon disk electrode (4 mm diameter) were employed

as the counter, reference, and working electrodes, respectively. To prepare the working electrode material, 2.5 mg of the catalysts and 20 μL of 5 wt% Nafion were dispersed in 980 μL of ethanol. After sonication for 30 min, 7.5 μL of the homogeneous ink was dropped onto the glassy carbon electrode. All potentials were quoted versus the reversible hydrogen electrode (RHE). The cyclic voltammetry (CV) curves were obtained in N_2-saturated 0.1 M $HClO_4$ with a scan rate of 50 mV s^{-1}. The ORR polarization curves were recorded in the O_2-saturated 0.1 M $HClO_4$ solution with a sweep rate of 10 mV s^{-1} at 1600 rpm. For the accelerated durability test (ADT), the CV and ORR polarization curves were measured after sweeping 10000, 20000, and 30000 cycles in the range of 0.6-1.1 V_{RHE} at a rate of 100 mV s^{-1}, together with a rotation speed of 1600 rpm, in an O_2-saturated 0.1 M $HClO_4$ solution at 25 °C. A commercial Pt/C (20 wt%) catalyst was also studied for comparison.

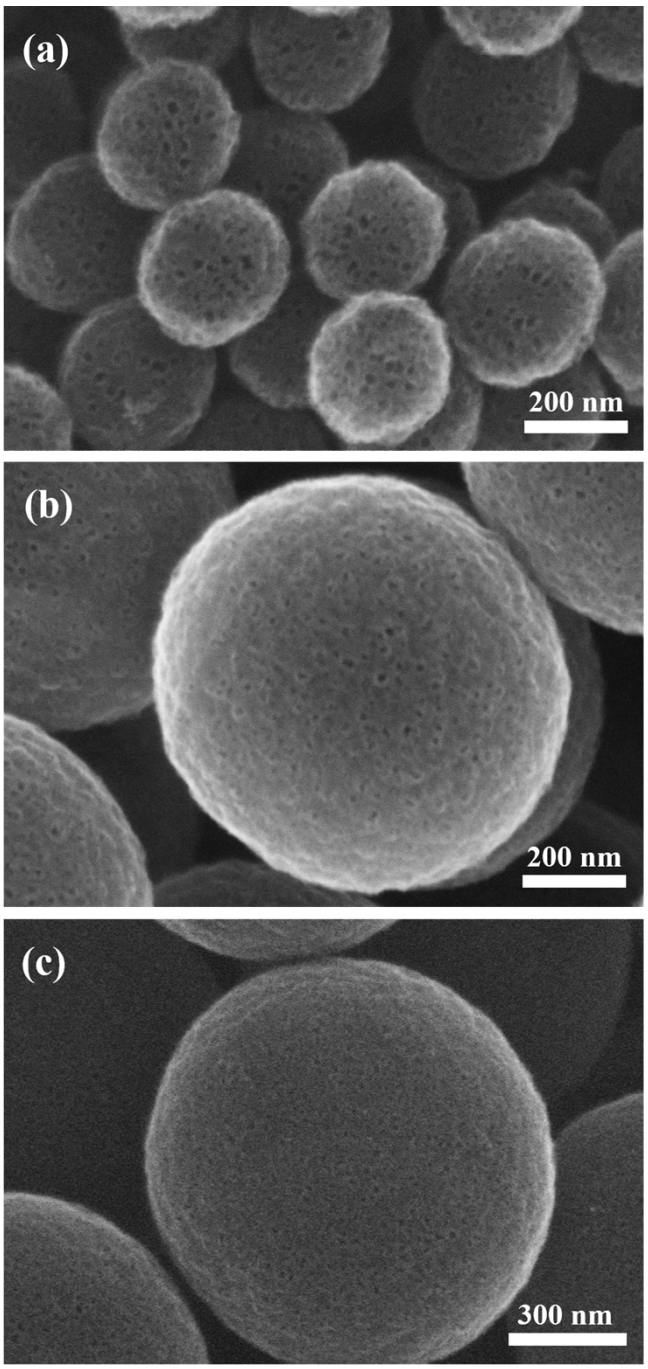

Fig. S1. SEM images of (a) HCS-W, (b) HCS and (c) HCS-E.

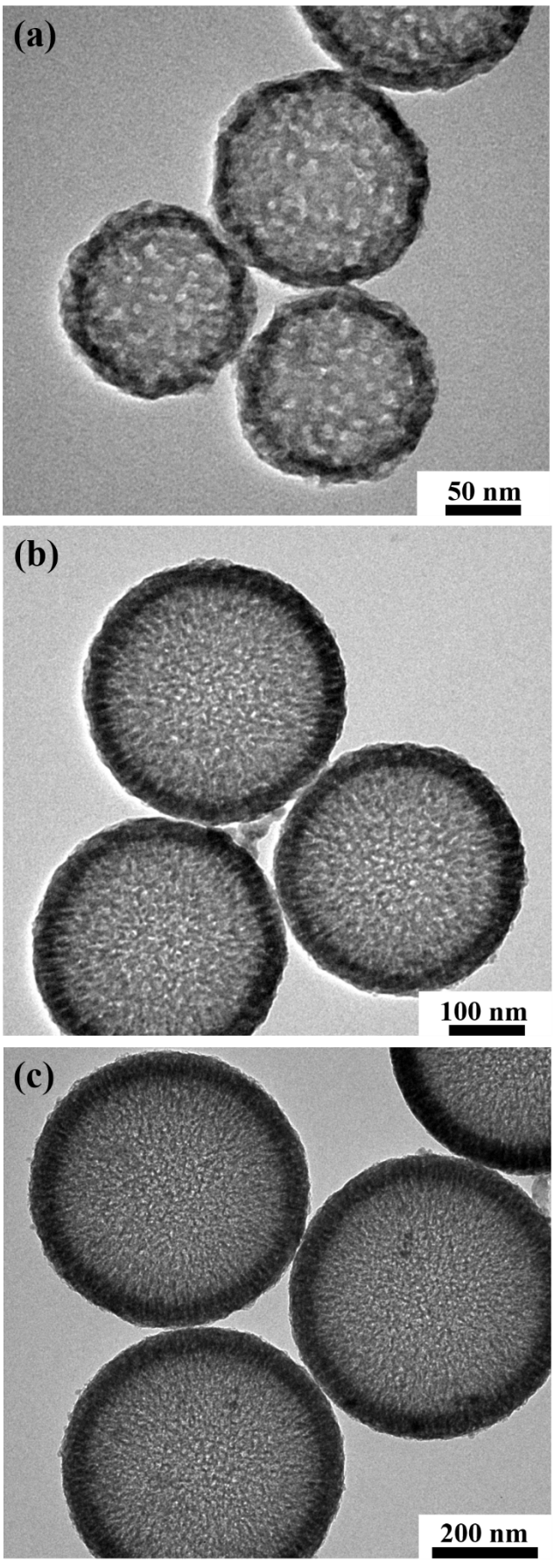

Fig. S2. TEM images of (a) HCS-W, (b) HCS and (c) HCS-E.

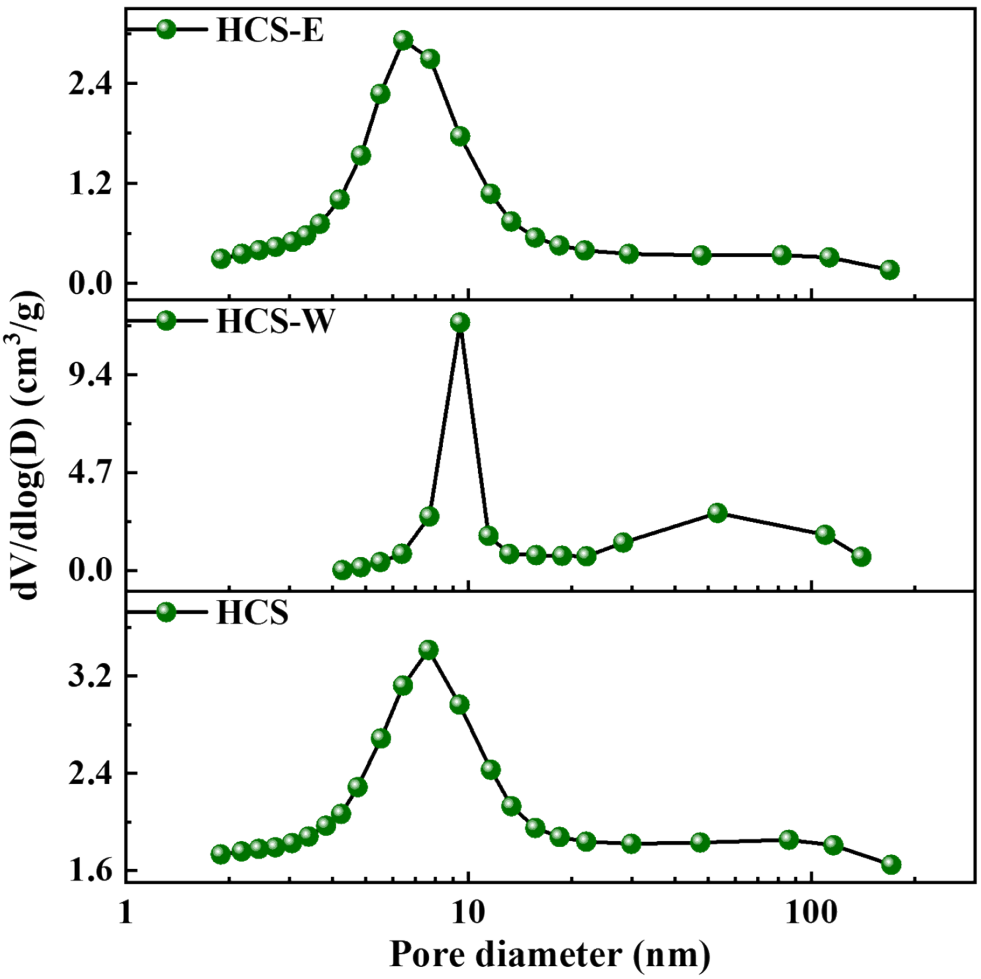

Fig. S3. Pore size distribution of HCS-E, HCS-W, and HCS.

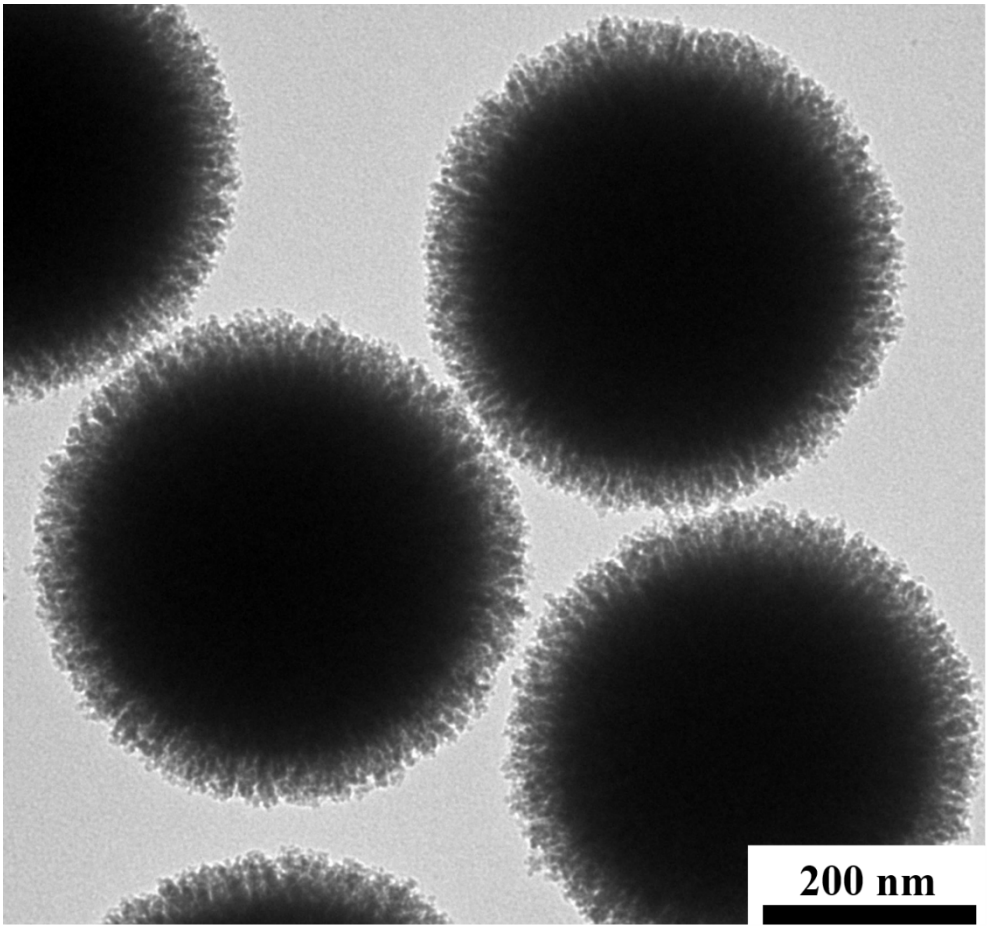

Fig. S4. TEM image of SiO_2@SiO_2 after calcination in air at 600 °C.

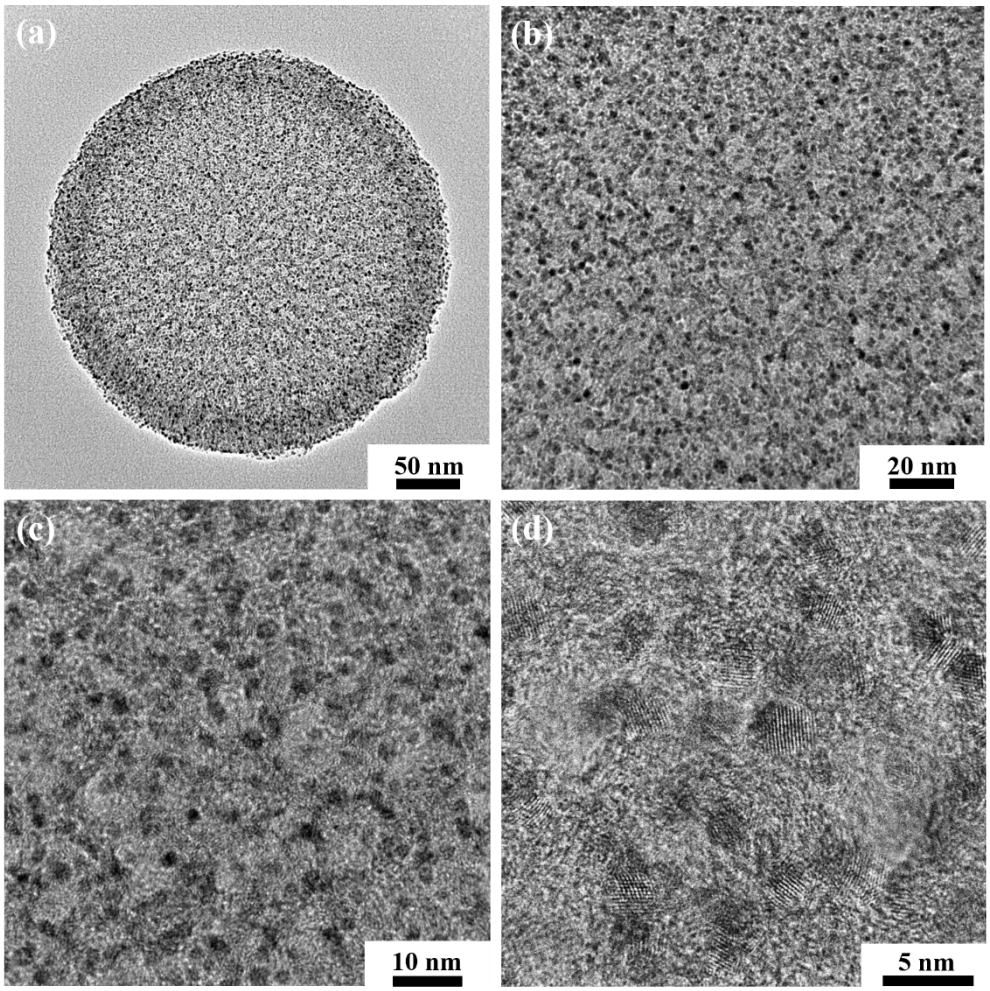

Fig. S5. (a-d) HRTEM images of Pt/HCS.

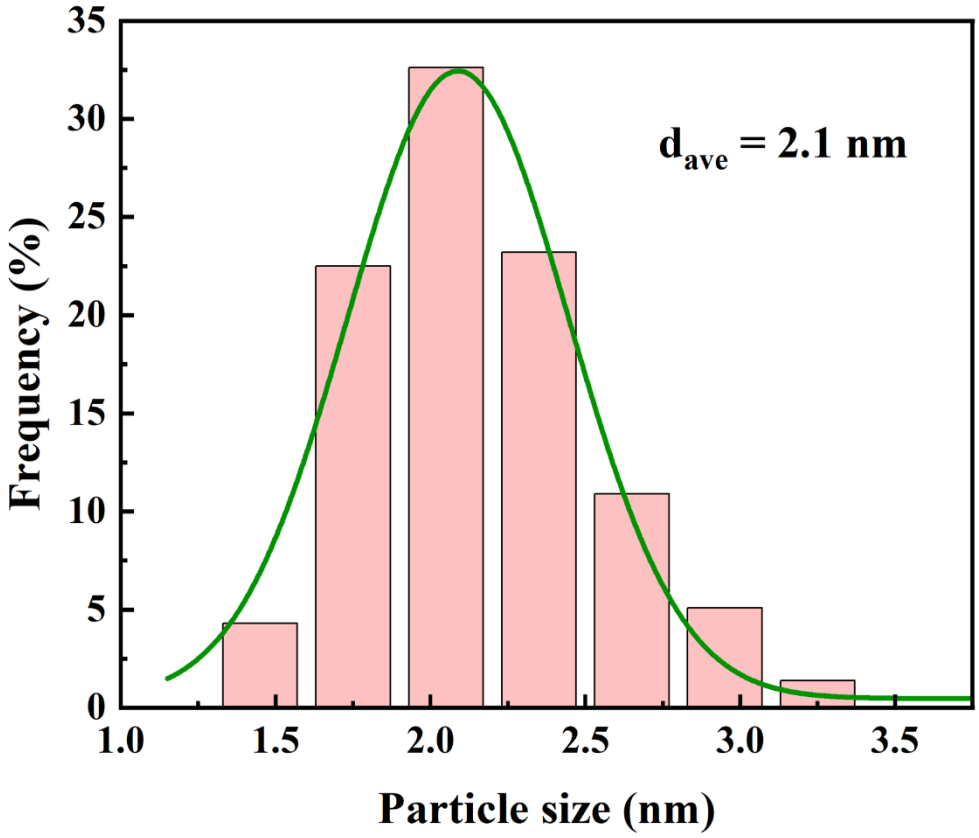

Fig. S6. Particle size distribution of Pt/HCS.

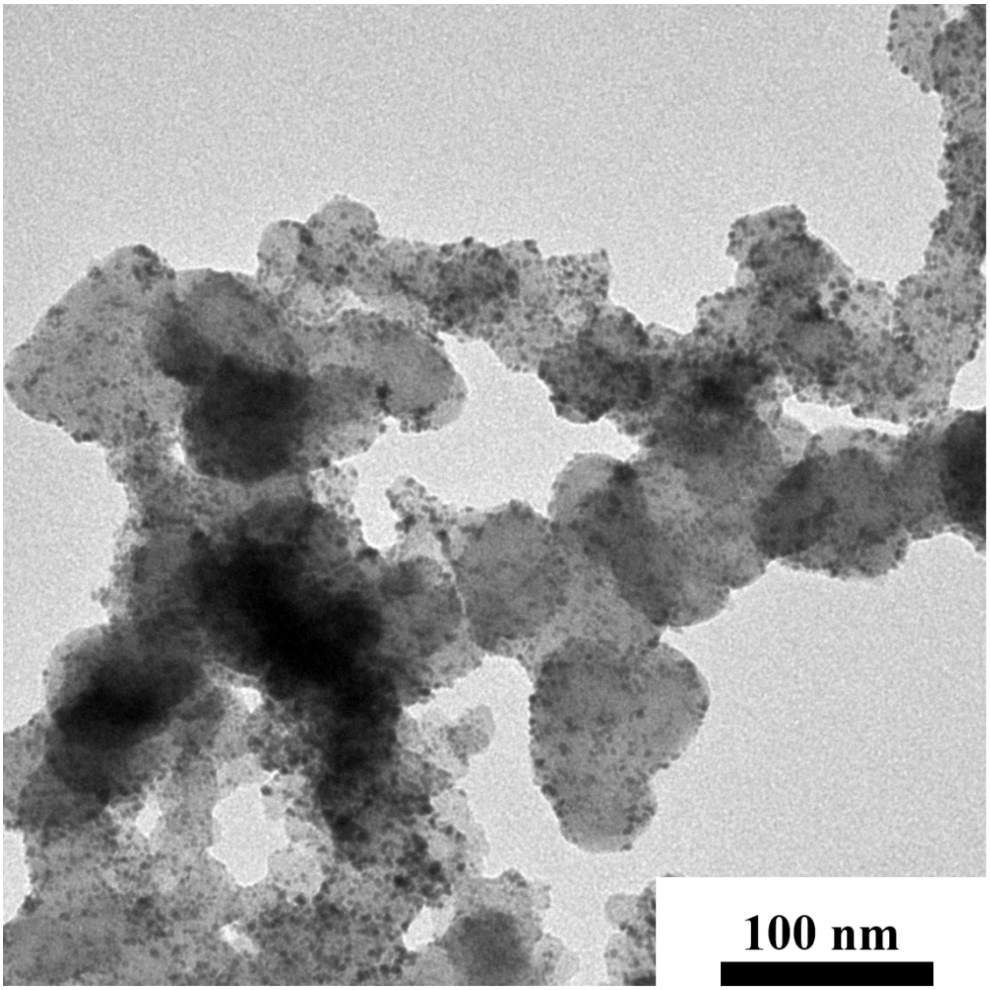

Fig. S7. TEM image of Pt/Vulcan.

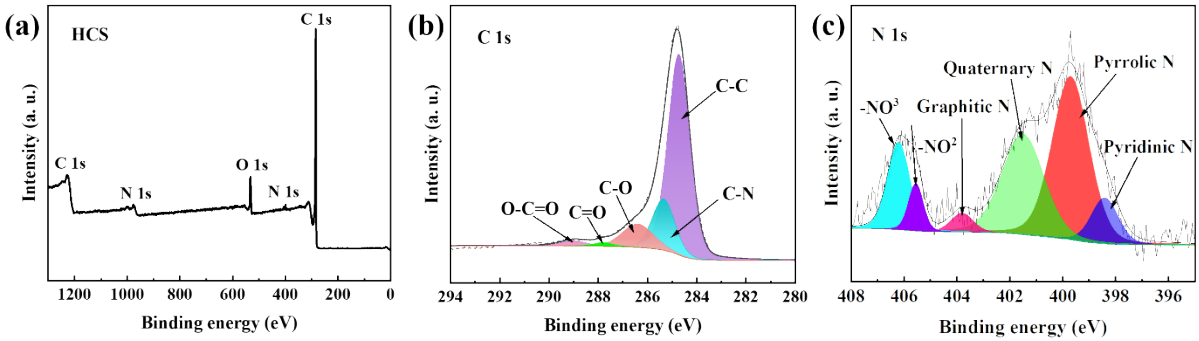

Fig. S8. (a) XPS survey, (b) C 1s, and (c) N 1s XPS spectra of N doped HCS.

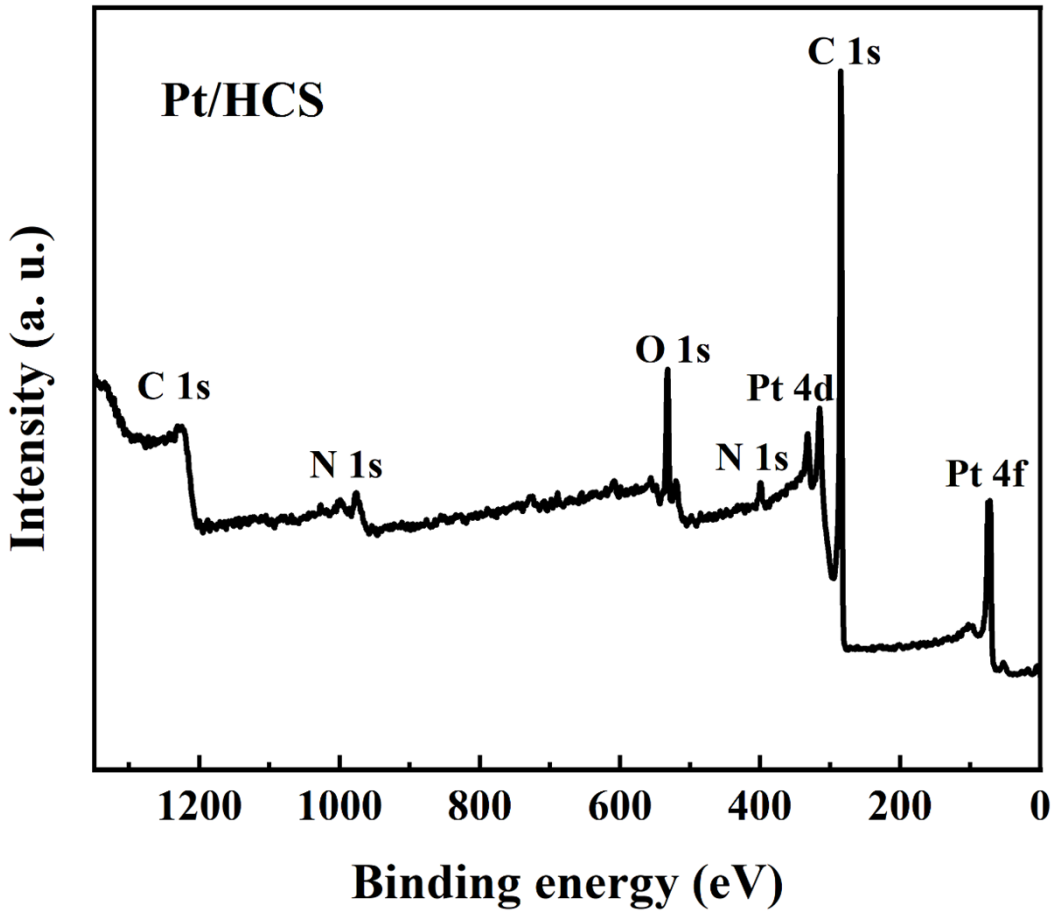

Fig. S9. XPS survey of Pt/HCS.

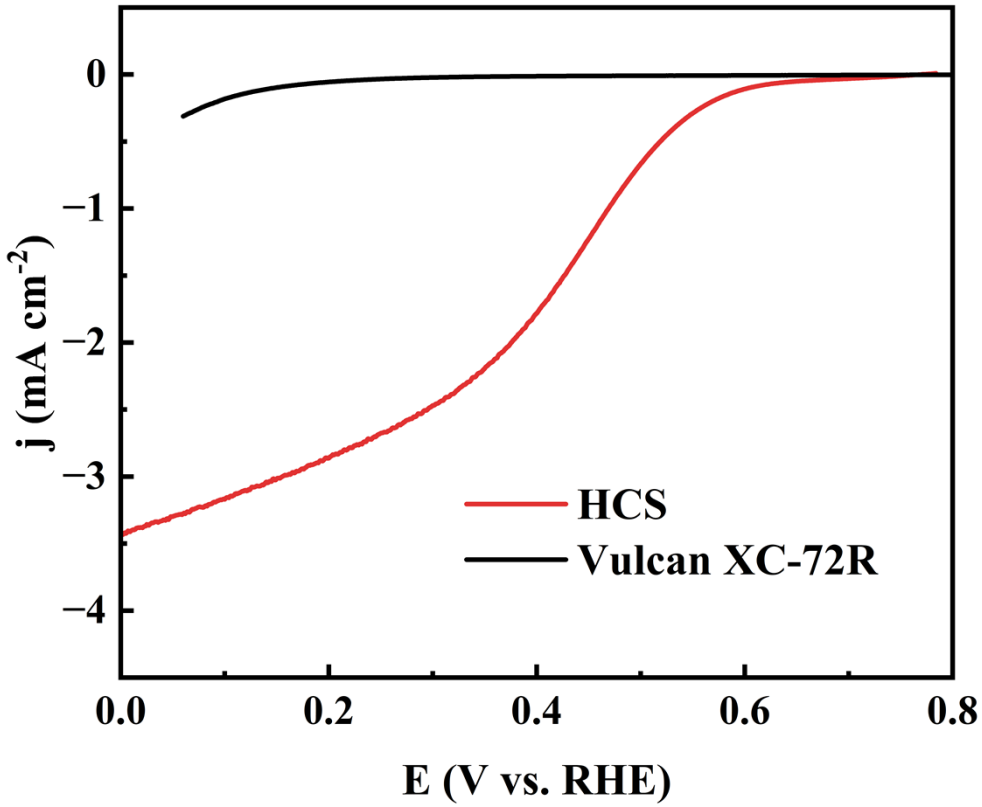

Fig. S10. ORR polarization curves of HCS and Vulcan XC-72R in an O_2-saturated $HClO_4$ solution.

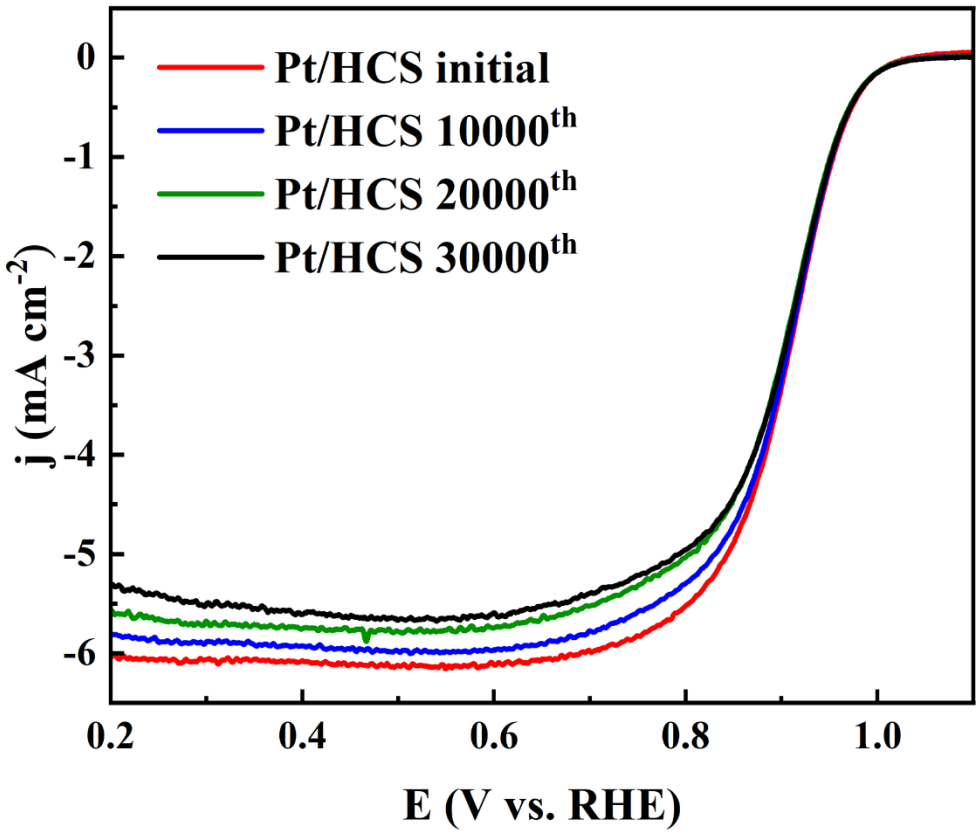

Fig. S11. ORR polarization curves of Pt/HCS after different potential cycles between 0.6 and 1.2 V.

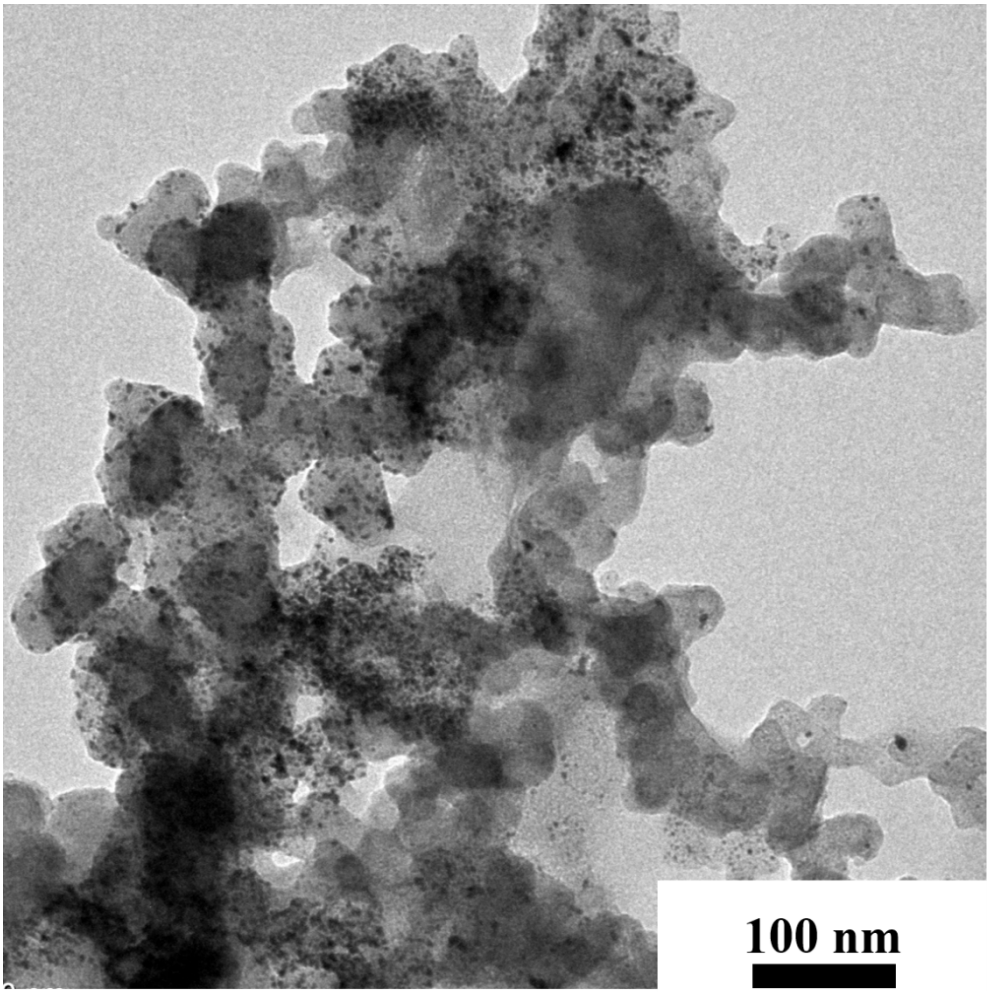

Fig. S12. TEM image of Pt/Vulcan after 30000 cycles.

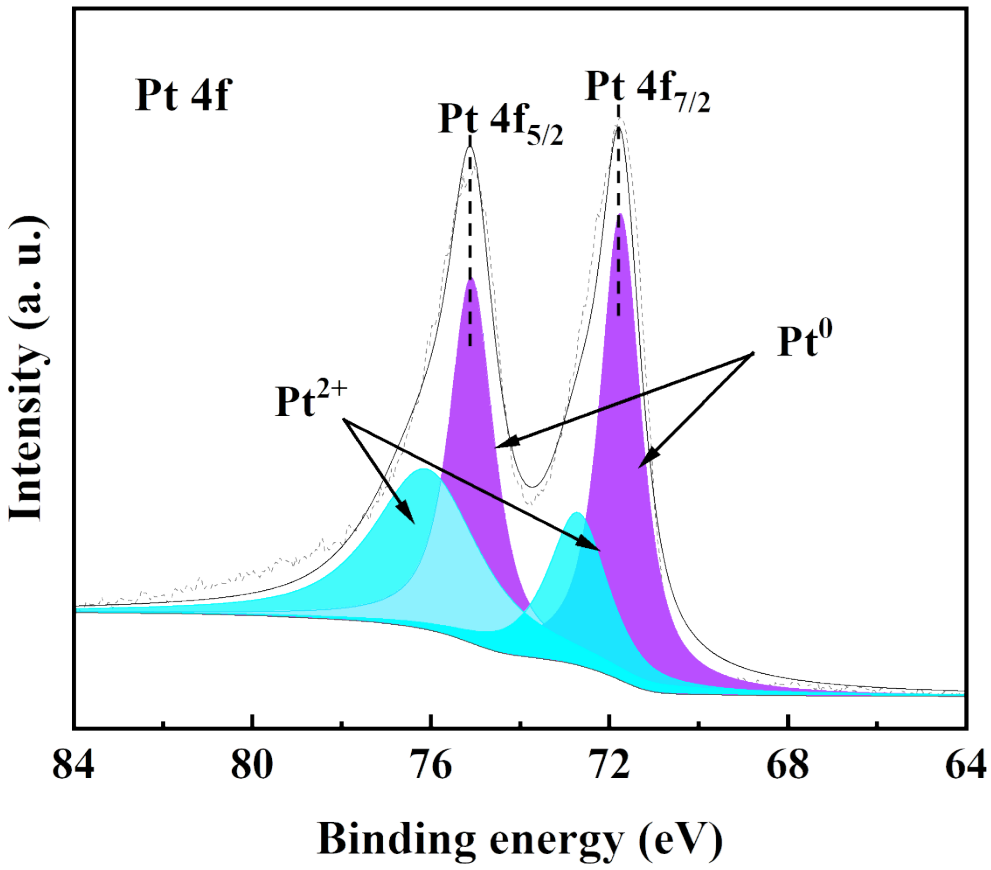

Fig. S13. Pt 4f XPS spectrum of Pt/HCS after 30000 cycles.

Table S1. The contents of Pt, N, C, and O in HCS and Pt/HCS.

Sample	Pt (at%)	N (at%)	C (at%)	O (at%)
Pt/HCS	2.29	2.77	85.58	9.15
HCS	-	2.28	90.76	6.96

Table S2. The contents of the different N species in Pt/HCS.

Sample	NO^3 (at%)	NO^2 (at%)	Graphitic N (at%)	Quaternary N (at%)	Pyrrolic N (at%)	Pyridinic N (at%)
Pt/HCS	2.6	2.8	4.8	18.1	51.5	20.2

Table S3. Comparison of ORR behavior on the Pt/HCS composite and various Pt-based electrocatalysts.

Catalysts	Mass activity ($mA\ mg^{-1}_{Pt}$)	Specific activity ($mA\ cm^{-1}_{Pt}$)	References
Pt/HCS	266	0.357	This work
Pt-N/C PMC	163	0.213	1
3ZIF-67-Pt/RGO	208	-	2
Pt/OVC	40	0.24	3
Pt@NC/C	116.5	-	4
Pt/C- TiO2	205	-	5
Pt/NH_2-graphene	172	0.29	6
Pt/PBI-graphene+FCB	183	-	7

[1] Y. Cheng, H. Lu, K. Zhang, F. Yang, W. Dai, C. Liu, H. Dong, X. Zhang, Fabricating Pt-decorated three dimensional N-doped carbon porous microspherical cavity catalyst for advanced oxygen reduction reaction, *Carbon*, 2018, **128**, 38-45.

[2] W. Wu, Z. Zhang, Z. Lei, X. Wang, Y. Tan, N. Cheng, X. Sun, Encapsulating Pt nanoparticles inside a derived two-dimensional metal-organic frameworks for the enhancement of catalytic activity, *ACS Appl. Mater. Interfaces*, 2020, **12**, 10359-10368.

[3] E. Teran-Salgado, D. Bahena-Uribe, P. A. Márquez-Aguilar, J. L. Reyes-Rodriguez, R. Cruz-Silva, O. Solorza-Feria, Platinum nanoparticles supported on electrochemically oxidized and exfoliated graphite for the oxygen reduction reaction, *Electrochim. Acta*, 2019, **298**, 172-185.

[4] J. Liu, W. Li, R. Cheng, Q. Wu, J. Zhao, D. He, S. Mu, Stabilizing Pt nanocrystals encapsulated in N-doped carbon as double-active sites for catalyzing oxygen reduction reaction, *Langmuir*, 2019, **35**, 2580-2586.

[5] J. Wang, M. Xu, J. Zhao, H. Fang, Q. Huang, W. Xiao, T. Li, D. Wang, Anchoring ultrafine Pt electrocatalysts on TiO_2-C via photochemical strategy to enhance the stability and efficiency for oxygen reduction reaction, *Appl. Catal. B-Environ.*, 2018, **237**, 228-236.

[6] L. Xin, F. Yang, S. Rasouli, Y. Qiu, Z.-F. Li, A. Uzunoglu, C.-J. Sun, Y. Liu, P. Ferreira, W. Li, Y. Ren, L. A. Stanciu, J. Xie, Pt nanoparticle anchoring on graphene supports through surface functionalization, *ACS Catal.*, 2016, **6**, 2642-2653.

[7] Z.- F. Li, L. Xin, F. Yang, Y. Liu, Y. Liu, H. Zhang, L. Stanciu, J. Xie, Hierarchical polybenzimidazole-grafted graphene hybrids as supports for Pt nanoparticle catalysts with excellent PEMFC performance, *Nano Energy*, 2015, **16**, 281-292.